Redundancy and Joint Limits of a Seven Degree of Freedom Upper Limb Exoskeleton

Levi Makaio Miller, Hyunchul Kim and Jacob Rosen

***Abstract*— The seven degree of freedom arm model is widely used in robotics, computer graphics, and much more. For wearable robotic systems, which are subject to joint limits, it is desirable to relate the joint limits to the redundantly of the system. A brief review of the arm model, redundant space and kinematics is presented. Following this review a closed form method is developed calculate the interval of the swivel angle (which characterizes the redundancy) that produces arm configurations that stay within joint limits.**

I. Introduction

Integrating capabilities of humans and robotic-machines into a unified system offers numerous opportunities for developing a new generation of assistive technology. The human machine interface (HMI) is a critical part of these system and for upper limb exoskeletons such as [1] proper modeling of the arm is a critical step. The seven degree of freedom (DoF) model is widely used for this purpose. Korein [2] was one of the first to study this model for the human arm and since then, many other researches have used it to study computer graphics [3] [4], redundant robots [5], upper limb exoskeletons [6] [7] [1] [8], biomechanics [9] [10] [11], and much more. The seven DoF model neglects translational and rotational motion of the scapula and clavicle but it gives a good combination of motion accuracy while reducing the model complexity. This model is redundant. Because exoskeletons have joint limits it is useful to relate the redundancy in the system to the joint limits of the device. This paper present a method to determine the range of the redundant degree of freedom that insures valid joint angles for the device.

II. Human Arm Model

The upper limb is a complex structure made up of rigid bone and soft tissue. Although much of the complexity is difficult to model, the overall arm movement can be represented by a simpler model composed of rigid links connected by joints. Three rigid segments, consisting of the upper arm, lower arm and hand connected by frictionless joints make up the simplified model. Figure 1(a) shows the rotation definitions of the model. The origin is located at the center of the shoulder joint. This joint has three intersection rotation and is responsible for shoulder abduction-adduction (abd-add), shoulder flexion-extension (flx-ext) and shoulder internal-external (int-ext) rotation. The upper and lower arm segments are attached by a single rotational joint at the elbow, creating elbow flx-ext. Finally, the lower arm and hand are connected by a three axis spherical joint resulting in pronation-supination (pron-sup), wrist flx-ext, and wrist radial-ulnar (rad-uln) deviation.

Levi Makaio Miller is a PhD Candidate in the Dept. of Mechanical Engineering, University of Washington, Seattle WA makaio@uw.edu

Hyunchul Kim is a PhD Candidate in the Dept. of Electrical Engineering, University of California Santa Cruz, Santa Cruz, CA hyunchul@soe.ucsc.edu

Jacob Rosen is an associate professor in the Dept. of Computer Engineering, University of California Santa Cruz, Santa Cruz, CA rosen@ucsc.edu

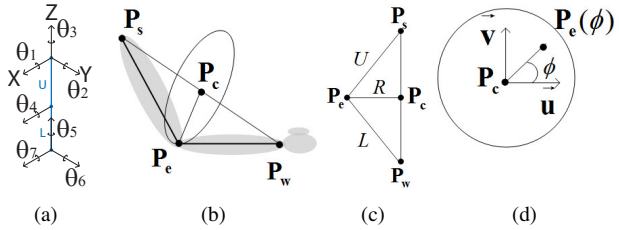

(a) (b) (c) (d)

Fig. 1. **(a)** Joint rotation definition for upper limb model. **(b)** The extra degree of freedom of the arm is defined by a rotation axis that goes from the shoulder to the wrist. **(c)** The shoulder, elbow and wrist form the triangle $P_s P_e P_w$. **(d)** A coordinate system allows the parameterizations of the elbow

III. The Extra Degree of Freedom

The seven DoF model is redundant, knowing the position and orientation of the hand does not fully specify the arm configuration. For an exoskeleton device where the entire arm is supported by the mechanism, knowing the full configuration of the arm is important. By additionally specifying the position of the elbow, the arm configuration is fully defined. With the position/orientation of the hand specified, it is possible to parameterize the elbow position as a function of a single variable. The arm creates a triangle with one point at the shoulder (P_s) one point a that the elbow (P_e) and the last point at the wrist (P_w). Both the shoulder and wrist joints are spherical, and allow rotation of P_e around the vector $(P_w - P_s)$ without changing the orientation or position of the hand [Fig. 1(b)].

Creating a local coordinate system at the center of the elbow circle (P_c), gives a reference to measure the swivel angle (ϕ) of the elbow. First create a normal vector that points in the same direction as $(P_w - P_s)$.

$$\vec{n} = \frac{P_w - P_s}{||P_w - P_s||} \tag{1}$$

Next project a vector onto the plane perpendicular to $\vec{n}$ and normalize. $\vec{u} = \frac{\vec{a} - (\vec{a}\cdot\vec{n})\vec{n}}{||\vec{a} - (\vec{a}\cdot\vec{n})\vec{n}||}$ where $\vec{a}$ can be selected as any vector. Badler and Torlani [12] suggest the selection of $\vec{a}$ to be the $-\vec{z}$ vector. To create the last vector of the coordinate system, take the cross product of $\vec{n}$ and $\vec{u}$, ($\vec{v} = \vec{n} \times \vec{u}$). Vectors $\vec{n}$, $\vec{u}$ and $\vec{v}$ form an orthonormal coordinate system. Where $\vec{u}$ and $\vec{v}$ are in the plane of the elbow circle [Fig. 1(d)]. The the radius (R) and center (P_c) of the circle are easily found through geometry.

$$R = U\sin(\alpha) \tag{2}$$

$$P_c = P_s + U\cos(\alpha)\vec{n} \tag{3}$$

$$\cos(\alpha) = \frac{L^2 - U^2 - ||P_w - P_s||^2}{-2U||P_w - P_s||} \tag{4}$$

Where U and L are the length of the upper and lower arm segments [Fig. 1(c)]. Now the position of the elbow can now be expresses as a parametrization of ϕ [13].

$$P_e(\phi) = R\left[\cos(\phi)\vec{u} + \sin(\phi)\vec{v}\right] + P_c \tag{5}$$

It is also possible to solve for ϕ given P_e. First project $P_e - P_s$ onto the plane of the elbow circle $\vec{p}_e = [(P_e - P_s) - (\vec{n}\vec{n}^T)(P_e - P_s)]$. Then:

$$\phi = atan2\left[\vec{n}^T(\vec{u} \times \vec{p}_e)\ ,\ \vec{u}^T\vec{p}_e\right] \tag{6}$$

IV. Forward Kinematics

Using the product of exponentials convention [14], [15] the forward kinematics are:

$$T_1T_2T_3T_4T_5T_6T_7g_{st} \quad = \quad g_d \tag{7}$$

with $T_i = \begin{bmatrix} R_i & P_i \\ 0 & 1 \end{bmatrix}$,where R_i is the 3×3 rotation matrix about the axis $\vec{\omega}_i$ and P_i equals $(P_{q_i} - R_iP_{q_i})$, when P_q is a point that the axis of rotation passes through. For the arm model: $\vec{\omega}_1 = [1,0,0]^T$, $\vec{\omega}_2 = [0,1,0]^T$, $\vec{\omega}_3 = [0,0,1]^T$, $\vec{\omega}_4 = [1,0,0]^T$, $\vec{\omega}_5 = [0,0,1]^T$, $\vec{\omega}_6 = [0,1,0]^T$, $\vec{\omega}_7 = [1,0,0]^T$ and $P_{q_{1,2,3}} = [0,0,0]^T$, $P_{q_4} = P_{e_0}$, $P_{q_{5,6,7}} = P_{w_0}$ with $P_{e_0} = [0,0,-U]^T$, $P_{w_0} = [0,0,-U-L]^T$

V. Inverse Kinematics

Equation (7) has seven unknowns and only six independent equations. To solve for the inverse kinematics with a closed form function an additional constraint must be imposed. The following function adds one additional independent equation when paired with eqn. (7)

$$T_1T_2P_{e_0} \quad = \quad P_e(\phi) \tag{8}$$

The two systems together are fully constrained. We will decompose (7) and (8) into one of two subproblems whose solutions are readily available.

A. Subproblem 1

Given the transformation matrix $T(\theta)$ Find θ such that:

$$T(\theta)P_0 \quad = \quad P_d \tag{9}$$

this corresponds to rotating an initial point P_0 about a given axis until it is coincident with P_d the desired final position. The soultion to this problem is:

$$\theta \quad = \quad atan2[\vec{\omega}^T(\vec{u} \times \vec{v}), \vec{u}^T\vec{v}] \tag{10}$$

$$\vec{u} \quad = \quad (P_0 - P_r) - \vec{\omega}\vec{\omega}^T(P_0 - P_r) \tag{11}$$

$$\vec{v} \quad = \quad (P_d - P_r) - \vec{\omega}\vec{\omega}^T(P_d - P_r) \tag{12}$$

Where $\vec{\omega}$ points in the direction of the rotation axis and P_r is a point the axis passes through. For the derivation refer to [14], [15]

B. Subproblem 2

Given the transformation matrix $T_i(\theta_i)T_j(\theta_j)$ where the rotation axis of T_i and T_j intersect, find θ_i and θ_j such that:

$$T_i(\theta_i)T_j(\theta_j)P_0 \quad = \quad P_d \tag{13}$$

this corresponds to rotating an initial point P_0 about the rotation axis of T_j by θ_j then about the rotation axis of T_i by θ_i, so that the final location of the point is coincident with P_d the desired final position. The solution to this problem is found by first finding P_g.

$$P_g \quad = \quad \alpha\vec{\omega}_i + \beta\vec{\omega}_j \pm \sqrt{\gamma}(\vec{\omega}_i \times \vec{\omega}_j) + P_r \tag{14}$$

$$\alpha \quad = \quad \frac{(\vec{\omega}_i^T\vec{\omega}_j)\vec{\omega}_j^T(P_0 - P_r) - \vec{\omega}_i^T(P_d - P_r)}{(\vec{\omega}_i^T\vec{\omega}_j)^2 - 1} \tag{15}$$

$$\beta \quad = \quad \frac{(\vec{\omega}_i^T\vec{\omega}_j)\vec{\omega}_i^T(P_d - P_r) - \vec{\omega}_j^T(P_0 - P_r)}{(\vec{\omega}_i^T\vec{\omega}_j)^2 - 1} \tag{16}$$

$$\gamma \quad = \quad \frac{||(P_0 - P_r)||^2 - \alpha^2 - \beta^2 - 2\alpha\beta\vec{\omega}_i^T\vec{\omega}_j}{||\vec{\omega}_i \times \vec{\omega}_j||^2} \tag{17}$$

where $\vec{\omega}_i$ and $\vec{\omega}_j$ point in the direction of the rotation axes of T_i and T_j and P_r is the point where the axes intersect. There may be zero, one or two real solution for P_g depending on γ. If solutions exist, then θ_i and θ_j can be found with subproblem one

$$T_i(-\theta_i)P_d \quad = \quad P_g \tag{18}$$

$$T_j(\theta_j)P_0 \quad = \quad P_g \tag{19}$$

For the derivation of this solution refer to [14], [15].

C. Decomposition of the Forward Kinematics

First θ_4 and can easily be solved by application of the law of cosine.

$$\theta_4 = \pi - \frac{L^2 + U^2 - ||w - s||^2}{2LU} \tag{20}$$

Equation (8) is already in the form of (13) with $P_0 = P_{e_0}$ and $P_d = P_e(\phi)$, and an immediate solution for θ_1 and θ_2 is available. Note that (13) has two solutions. For a natural arm configuration the negative sign in (14) should be chosen. Next solve for θ_3. First premultiply equation (7) by $(T_1T_2)^{-1}$ and post multiply by $g_{st}^{-1}P_{w_0}$. Since P_{w_0} is an eigne vector of T_5, T_6 and T_7 with eigne value one, $T_5T_6T_7P_{w_0} = P_{w_0}$

$$T_3(T_4P_{w_o}) = (T_1T_2)^{-1}g_dg_{st}^{-1}P_{w_0} \tag{21}$$

This is in the form of (9) when $P_0 = (T_4P_{w_0})$ and $P_d = (T_1T_2)^{-1}g_dg_{st}^{-1}P_{w_0}$. Solving for θ_5 and θ_6, being by premultiplying equation (7) by $(T_1T_2T_3T_4)^{-1}$ and post multiply by $g_{st}^{-1}P_7$. where $P_7 = [1,0,-U-L]^T$ which is an eigne vector of T_7 with an eigne value of one, so $T_7P_7 = P_7$

$$T_5T_6P_7 = (T_1T_2T_3T_4)^{-1}g_dg_{st}^{-1}P_7 \tag{22}$$

This is now in the form of (13) when $P_0 = P_7$ and $P_d = (T_1T_2T_3T_4)^{-1}g_dg_{st}^{-1}P_7$. Equation (13) has multiple solution. The negative sign in (14) should be chosen. Finally solve for θ_7. Begin by premultiplying by $(T_1T_2T_3T_4T_5T_6)^{-1}P_s$ and post multiplying $g_{st}^{-1}P_s$

$$T_7P_s = (T_1T_2T_3T_4T_5T_6)^{-1}g_dg_{st}^{-1}P_s \tag{23}$$

this is in the form of (9) where $P_0 = P_s$ and $P_d = (T_1T_2T_3T_4T_5T_6)^{-1}g_dg_{st}^{-1}P_s$

VI. Joint Limits

Wearable robotic system are subject to joint limitation and it is desirable to relate the swivel angle to the joint limits. This can be accomplished by calculating the values of ϕ where the joints are at their limits to determine boundaries for the intervals of valid swivel angles. Due to the symmetry of the model, joints five, six and seven are found in a similar manner as joints one, two and three. Therefore only a treatment of the first three joints is presented.

Step 1: Calculate β

Depending on the desired location of P_w there are three different types of solution sets. To determine which set the problem is in, calculate β, the angle between the the vectors $\vec{n}$ and $\vec{\omega}_1$:

$$\beta \quad = \quad acos(\vec{\omega}_1^T\vec{n}) \tag{24}$$

The three case, shown in fig. 2, correspond to when $\beta > \alpha$, $\beta = \alpha$, and $\beta < \alpha$. The first case ($\beta > \alpha$) is the most common and occurs when the first rotation axis ($\vec{\omega}_1$) is outside the elbow circle. The next case ($\beta = \alpha$) is the least common and occurs when $\vec{\omega}_1$ pierces the perimeter of the elbow circle. In this configuration there is a value of ϕ that puts the device into a singular position. The last case ($\beta < \alpha$) occurs when $\vec{\omega}_1$ is inside the elbow circle.

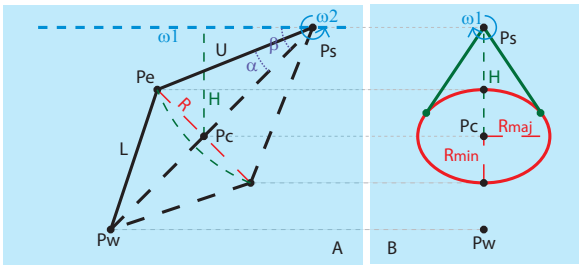

(a) $\beta > \alpha$

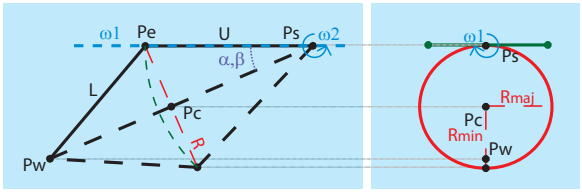

(b) $\beta = \alpha$

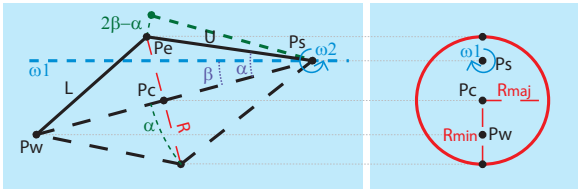

(c) $\beta < \alpha$

Fig. 2. Planes A and B are normal to the vectors ω_2 and ω_1 respectively and both pass through the point P_s. **(a)** When $\beta > \alpha$ the range of θ_1 is the angle between the lines that pass through P_s and are tangent to the elliptical projection of the elbow circle. The range of θ_2 is equal to 2α. **(b)** When $\beta = \alpha$ the point P_s is on the projection of the elbow circle and the angle of the tangent lines is π, note that the device will be singular for some value of ϕ in this configuration. The range of θ_2 is 2α. **(c)** When $\beta < \alpha$ the point P_s is inside the projection of the elbow circle and the lines passing through this point will never be tangent to the ellipse. The range of θ_1 is 2π. The range of θ_2 will be $\alpha + 2\beta - \alpha = 2\beta$.

Step 2: Calculate Joint Minimum and Maximum

For a particular P_w the range of each joint as ϕ rotates in the interval $[0, 2\pi]$ will be equal to 2π or less then or equal to π. The exact minimum and maximum can be computed by establishing a reference angle within the joints range of motion and calculating the deviation from that reference.

Reference Angle: A convenient reference angle for θ_1 and θ_2 is the angle formed by them when the elbow is located at $P_{e_r} = (U\,\vec{n})$. This corresponds to when the elbow is on the line that is colinear with the one going from P_s to P_w. The references (θ_{1_r},θ_{2_r}), can be found by solving the following equation:

$$T_1 T_2 P_{e_0} \quad = \quad P_{e_r} \tag{25}$$

This equation is in the form of (13) and can be immediately solved. This has multiple solutions, chose the negative sign in (14) to be consistent with the earlier selections. The reference angle θ_{3_r} will be $\frac{\pi}{2}$ when $P_{w_x} < 0$ and $-\frac{\pi}{2}$ when $P_{w_x} \geq 0$.

Joint Range: The range of each joint depends on the value of β. The value of the range can be determined through geometry (fig. 2). $\Delta\theta_1$ is the angle of the line that passes through P_s and is tangent to the elliptical projection of the elbow circle onto the plane normal to $\vec{\omega}_1$. $\Delta\theta_2$ is the angle of between the line P_{e_r}, and $\Delta\theta_3$ (not pictured) is the angle between the projection of an ellipse onto the

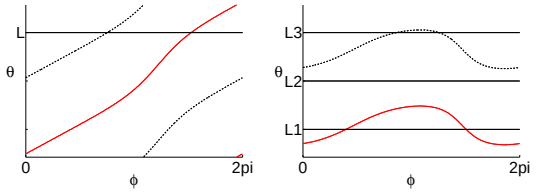

(a) (b)

Fig. 3. Intersection of joint limit L with θ, the dashed black and solid red lines represent the multiple possible solution for the inverse problem. **(a)** If the joint range is equal to 2π both the valid and invalid solution set for θ will interest the joint limit L exactly once each. In this case you must chose the valid solution. **(b)** If the joint range is less then 2π there are three possible intersection cases. 1)The joint limit $L1$ intersects the valid solution for θ in two places (possibly a double root). This makes 2 real and valid solution. 2)The joint limit $L2$ dose not intersect either solution. This makes two imaginary solutions. 3)The joint limit $L3$ intersects the invalid solution for θ in two places. This makes two real but invalid solutions.

plane normal to $\vec{\omega}_3$ in a similar manner to $\Delta\theta_1$. when $\beta > \alpha$

$$\Delta\theta_1 = \pm atan\left(\sqrt{\frac{R_{1_{maj}}^2}{H_1^2 - R_{1_{min}}^2}}\right) \tag{26}$$

$$\Delta\theta_2 = \pm\alpha \qquad \Delta\theta_3 = \pm\pi \tag{27}$$

Where $H_1 = ||P_c - \vec{\omega}_1^T \vec{\omega}_1 P_c||$ which is the magnitude of the projection of P_c onto a plane normal to $\vec{\omega}_1$, $R_{1_{maj}} = R$ and $R_{1_{min}} = Rcos(\beta)$ are the major and minor axes of the ellipse(fig. 2(a)). For $\Delta\theta_3$ P_s is inside the projection of the ellipse and no line is tangent. When $\beta = \alpha$ (fig. 2(b))

$$\Delta\theta_1 = \pm\frac{\pi}{2} \qquad \Delta\theta_2 = \pm\alpha \qquad \Delta\theta_3 = \pm\frac{\pi}{2} \tag{28}$$

In this case the point of reference for both ellipses are on the ellipse and the tangent line is $\frac{\pi}{2}$. When $\beta < \alpha$ (fig. 2(c))

$$\Delta\theta_1 = \pm\pi \qquad \Delta\theta_2 = \pm\alpha \mp (2\beta - \alpha) \tag{29}$$

$$\Delta\theta_3 = atan\left(\sqrt{\frac{R_{3_{min}}^2}{H_3^2 - R_{3_{maj}}^2}}\right) \tag{30}$$

Where $H_3 = Wsin(\alpha) + \left[\frac{Wsin(\beta)}{2cos(\alpha+\beta)} - \frac{Wsin(\beta)}{2cos(\alpha-\beta)}\right]$. $R_{3_{maj}} = \left[\frac{Wsin(\beta)}{2cos(\alpha-\beta)} + \frac{Wsin(\beta)}{2cos(\alpha+\beta)}\right]$ and $R_{3_{min}} = R_{3_{maj}}\sqrt{1 - \left(\frac{sin(\alpha)}{cos(\beta)}\right)^2}$. the top sign in $\Delta\theta_2$ will used when $P_{w_x} > 0$ otherwise the bottom sign is selected.

Step 3: Joint Limit Intersection

Determining the value(s) of ϕ that result in the joint being equal to the joint limits (L_i), will establish the boundaries for the interval of ϕ that will result in valid joint configurations. There will be four solutions for each joint (two for the maximum and two for the minimum limit), but not all solutions will be valid.

Valid Solution: There are four possible case. The first case is when the range of θ is 2π. In this case there will always be one real, valid solution, and one real, invalid solution for each limit. The invalid solution represents the intersection with θ from the unselected IK solutions from eqn. (7) and (8). This case is represented in fig. 3(a). The other three cases are when the range of θ is less then or equal to π. Then, there may be 2 real (possibly double root) valid solutions, 2 real invalid solutions, or 2 imaginary invalid solutions. The two real invalid solutions are from the intersections of θ with the unselected IK solutions, and the

imaginary solution represent when neither the selected or unselected IK solution intersect with L_i. Figure 3(b) shows the last three cases. If the joint limit is within the range of the joint:

$$(\theta_{i_r} - \Delta\theta_i) \quad \geq \quad L_i \quad \geq \quad (\theta_{i_r} + \Delta\theta_i) \tag{31}$$

then the solutions are valid. Once it is determined how many of the solutions are valid the values need to be calculated.

Calculate Intersection Values: To calculate ϕ such that θ_i is equal to L_i set θ_i equal to L_i and solve eqn. (7). This equation is not redundant with one joint angle selected. For the first three joints, we will begin by decomposing (7) by postmultiplying by $g_{st}^{-1}P_{w_0}$. Since P_{w_0} is an eigen vector of the last three joints with an associated eigen value of one, (7) becomes:

$$T_1T_2T_3T_4P_{w_0} \quad = \quad g_d g_{st}^{-1} P_{w_0} = P_w \tag{32}$$

This equation can further be decomposed to the form of (13) once θ_i is set to L_i, which will allow for the immediate solution of $\theta_{1_{Li}}$ and $\theta_{2_{Li}}$ which are the angles of joints one and two at joint limit L_i. Then ϕ_{Li} can be solved using eqn. (8) and (6).

L_1 - Given the joint limit L_1, the matrix T_1 is constant. By premultiply (32) by T_1^{-1} we get:

$$T_2T_3(T_4P_{w_0}) \quad = \quad (T_1^{-1}P_w) \tag{33}$$

Which is in the form of (13). Where $P_0 = (T_4P_{w_0})$, $P_d = (T_1^{-1}P_w)$, The rotation intersection is P_s and the rotation axes are $\vec{\omega}_2$ and $\vec{\omega}_3$. If $\beta \geq \alpha$ then both solution to (33) will be valid if eqn (31) is satisfied for $i = 1$. If $\beta < \alpha$, then the positive sign in (14) represents the valid solution.

L_2 - Given the joint limit L_2, the matrix T_2 is constant. By preforming a change of coordinates on T_2, eqn. (32) can put in the form of (13)

$$T_1T_{23}(T_2T_4P_{w_0}) \quad = \quad (P_w) \tag{34}$$

$$T_{23} \quad = \quad T_2T_3T_2^{-1} \tag{35}$$

Where $P_0 = (T_2T_4P_{w_0})$, $P_d = P_w$, the intersection location is P_s and the rotation axis are $\vec{\omega}_1$ and $R_2\vec{\omega}_3$. If eqn. (31) is satisfied for $i = 2$, then both solutions to (34) will be valid.

L_3 - Given L_3 the matrix T_3 is constant and eqn, (32) is already in the form of (13).

$$T_1T_2(T_3T_4P_{w_0}) \quad = \quad (P_w) \tag{36}$$

Where $P_0 = (T_3T_4P_w)$, $P_d = (P_w)$, The rotation intersection is P_s and the rotation axes are $\vec{\omega}_1$ and $\vec{\omega}_2$. If $\beta \leq \alpha$ then both solution to (33) will be valid if eqn (31) is satisfied for $i = 3$. If $\beta > \alpha$, then the negative sign in (14) represents the valid solution.

After the intersection are found that define intervals of ϕ, we must determine which intervals are invalid, and which of the valid intervals we would like to work in.

Step 4: Intervals

For each joint there is up to four valid solutions for ϕ_{Li}. These solutions mark the boundary between the intervals of ϕ that result in valid joint configurations and those that result in joint configurations that are out side joint limits. Because ϕ wraps around at 2π the number of intervals will be equal to the number of valid solutions for ϕ_{Li}. The intervals will alternate between valid and invalid, so testing one value of ϕ is enough to determine which of the intervals are valid. Taking the intersection of every valid set for each of the six joints, results in a single valid set of intervals of ϕ where all joints limits are mutually satisfied (fig. 4). Because the functions are continuous, it is not possible to jump from one interval to another unless you are in a singular position. After selecting an initial position the robot is restricted to live in a particular interval within the set.

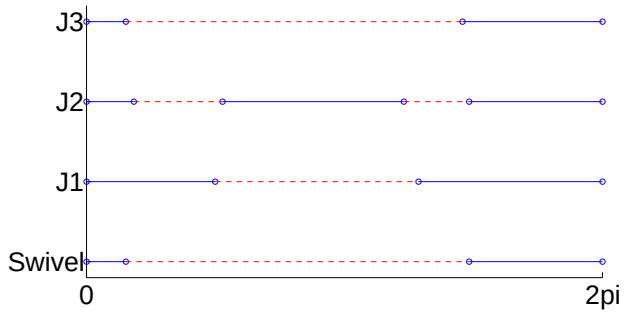

Fig. 4. Value of ϕ that produce valid joint limits (solid blue) and invalid joint limits (dashed red). The valid interval of the swivel angle is the intersection of the valid intervals of ϕ for each joint.

VII. Discussion

This paper presented a review of a commonly used seven DoF arm model. This was followed by a brief treatment of the redundant space and kinematics. A four step process consisting of 1) calculating β 2) calculating joint minimum and maximums 3) Finding joint limit intersections and 4) choosing valid intervals is developed as a closed form method to find the range of the swivel angle that results in all joint limits being satisfied.

References

[1] J. Rosen and J. C. Perry, "Upper limb powered exoskeleton," *International Jornal of Humanoid Robotics*, vol. 4, no. 3, pp. 529–548, 2007.

[2] J. U. Korein, *A Geometric Investigation of Reach*. MIT Press, 1985.

[3] M. Kallmann, "Analytical inverse kinematics with body posture control," *Computer Animation and Virtual Worlds*, 2007.

[4] P. Lee, S. Wei, J. Zhao, and N. I. Badler, "Strength guided motion," *Computer Graphics*, vol. 24, no. 4, pp. 253–262, 1990.

[5] I. Iossifidis and A. Steinhage, "Controlling a redundant robot arm by means of a haptic sensor," in *ROBOTIK 2002, Leistungsstand - Anwendungen - Visionen*, 2002, pp. 269–274.

[6] J. C. Perry and J. Rosen, "Design of a 7 degree-of-freedom upper-limb powered exoskeleton," in *IEEE/RAS-EMBS International Conference on Biomedical Robotics and Biomechatronics*, 2006.

[7] J. C. Perry, J. Rosen, and S. Burns, "Upper-limb powered exoskeleton design," *Mechatronics*, vol. 12, no. 4, pp. 408–417, 2007.

[8] N. Tsagarakis and D. G. Caldwell, "Development and control of a 'soft-actuated' exoskeleon for use in physiotherapy and training," *Autonomous Robots*, vol. 15, pp. 21–33, 2003.

[9] X. Wang, "A behavior-based inverse kinematics algorithm to predict arm prehension posture for computer-aided ergonomic evaluation," *Journal of Biomechanics*, vol. 32, pp. 453–460, 1999.

[10] X. Zhang and D. B. Chaffin, "The effects of speed variation on joint kinematics during multisegment reaching movements," *human movement science*, vol. 18, pp. 741–757, 1999.

[11] F. Yang and X. Yuan, "An inverse kinematical algorithm for human arm movement with comfort level taken into account," in *IEEE Conference on Control Applications*, vol. 2, 2003.

[12] N. I. Badler and D. Tolani, "Real-time inverse kinematics of the human arm," *Presence*, vol. 5, no. 4, pp. 393–401, 1996.

[13] D. Tolani, A. Goswami, and N. I. Badler, "Ral-time inverse kinematics techniques for anthropomorphic limbs," *Graphucal Models*, vol. 62, pp. 353–388, 2000.

[14] R. M. Murray, Z. Li, and S. S. Sastry, *A Mathematical Introduction to Robotic Manipulation*. CRC Press, 1994.

[15] G. Yan, "Decomposible closed form inverse kinematics for reconfigurable robots using product-of-exponentials formula," Master's thesis, Nanyang Technological University, 2000.